Available online on www.ijddt.com
International Journal of Drug Delivery Technology 2018; 8(4); 187-196
doi: 10.25258/ijddt.8.4.6

ISSN: 0975 4415

Research Article

Formulation and Evaluation of *β*-Cyclodextrin Grafted Chitosan Nanocomposites for Controlled release of Anticancer Drug Cyclophosphamide

Umakanta Sahoo[1], Mira Das[1], Padmolochan Nayak[2*]

[1]*Department of Chemistry, Institute of Technical Education and Research, Siksha 'O' Anusandhan University, Bhubaneswar, Odisha, India*
[2]*Synergy Institute of Technology, Odisha, India*

Received: 14th May, 18; Revised: 3rd Oct, 18, Accepted: 10th Nov, 18; Available Online: 25th Dec, 2018

ABSTRACT

In this paper *β* -cyclodextrin (β-CD) grafted chitosan (CS) with MMT was different feed ratio known as (β-CD-g-CS/MMT). The prepared nanocomposites were characterized by XRD, FTIR, SEM, TGA, TDC and swelling in stimulated in different biological fluid. The model drug Cyclophosmide (CYC) was used for controlled drug delivery purpose. From FTIR result was clearly demonstrated that the model drug CYC did not change in any molecular level at β-CD-g-CS/MMT (i.e. at <10 nm scale). Additionally, in DSC result, CYC was interacted with nanocomposites at scale >100 nm level. In vitro drug release system was carried out by Korsmeyer Peppas's power law. CYC and other drugs like Doxorubicin (DOX) and Curcumin (CUM) were presented exceptional higher drug result in different pH medium. It was observed that CS/MMT was decrease less drug release rate compared to β-CD-g-CS/MMT. So that it can be clearly understood that β-CD-g-CS/MMT grafted nanocomposites have enhanced drug release activity in different pH medium.

Keyword: β-cyclodextrin, Chitosan, MMT, Nanocomposites, Cyclophosphamide, Drug delivery system.

INTRODUCTION

Chitosan (CS) is a biopolymer which is used for different purpose like biomedical, cosmetics, pharmaceutical products etc. It is very popular in pharmaceutical and medical filed for its unique properties like biodegradable, non toxic, biocompatible, antimicrobial activities etc. In present research, it is used for drug delivery applications[1]. Most of scientific research publications have been proved; CS can be use for oral drug delivery purpose. But its poor physical properties such as brittleness, poor solubility require improvement for more medical application particular in drug delivery field as carrier matrix. Many researchers have been reported that, in chemical and biochemical routs will be possible to improve the expected properties. Among grafting procedure, it is easy to prepare and synthesis of modified chitosan polymer composites with biodegrable nature for different purpose[2].

Chitosan nanocomposites have been well studied for drug delivery and other applications using MMT nanoclay. But limited studies have been made on chitosan grafted onto *β* –cyclodextrin for drug delivery purpose[2-6]. Generally the hydrophobicity and hydrophilicity nature of polymer is contributing a lot in controlling the drug release characteristics apart from its flexibility[7-10]. However this experiment is focused on the preparation of chitosan nanocomposites grafted with *β* –cyclodextrin for controlled drug release of anticancer drug CYC in different pH medium.

This work is aimed to prepare *β* -cyclodextrin grafted chitosan (CS) with MMT to evaluate the feasibility of loading and release of CYC drug with applicable efficiency and to elucidate the effect of biopolymer addition and MMT clay addition on the rate of CYC drug release.

MATERIALS

Chitosan (Mw = 110 kDa, deacetylation degree>90%) and β-cyclodextrin (β-CD) were obtained Himedia. MMT and Cyclophosphamide was purchased from Hindhustan scientific Cuttack, Odisha. All other chemicals used were of analytical grade which were commercially available.

Preparation of CH/ MMT nanocomposites

Dry weight CS was dissolved in 2% v/v aqueous glacial acetic acid at a concentration of 2 Wt%. The prepared solution samples were subjected to centrifuging at 2000 rpm to remove the insoluble residual material[11]. In addition, MMT was swelled in 50 ml distilled water by magnetic stirring for 60 min at 30 ± 1ºC. Then the prepared chitosan solution with chitosan/MMT Wt ratio of 1/1, 1/2 and 2/1, followed by stirring for 4 h under different temperature (40º, 50º, 60º and 70ºC.) Then, CS/MMT solutions were filtered and dried by vacuum at 70ºC for 48 hours.

Synthesis of β-cyclodextrin grafted with CS/MMT (CD-g-CS/MMT)

The β-CD-g-CS/MMT was prepared by the following procedure. Chitosan/MMT was prepared in 1% (v/v) acetic

Author for Correspondence: sahooumakanta48@gmail.com

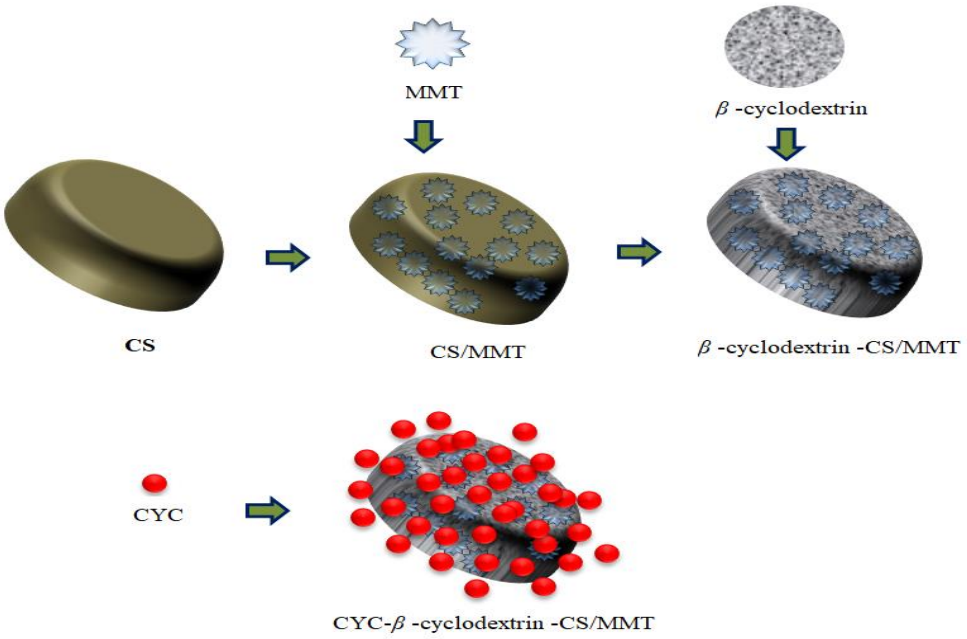

Figure 1: Schematically representation of *β*-cyclodextrin grafted chitosan nanocomposites for controlled release of anticancer drug Cyclophosphamide.

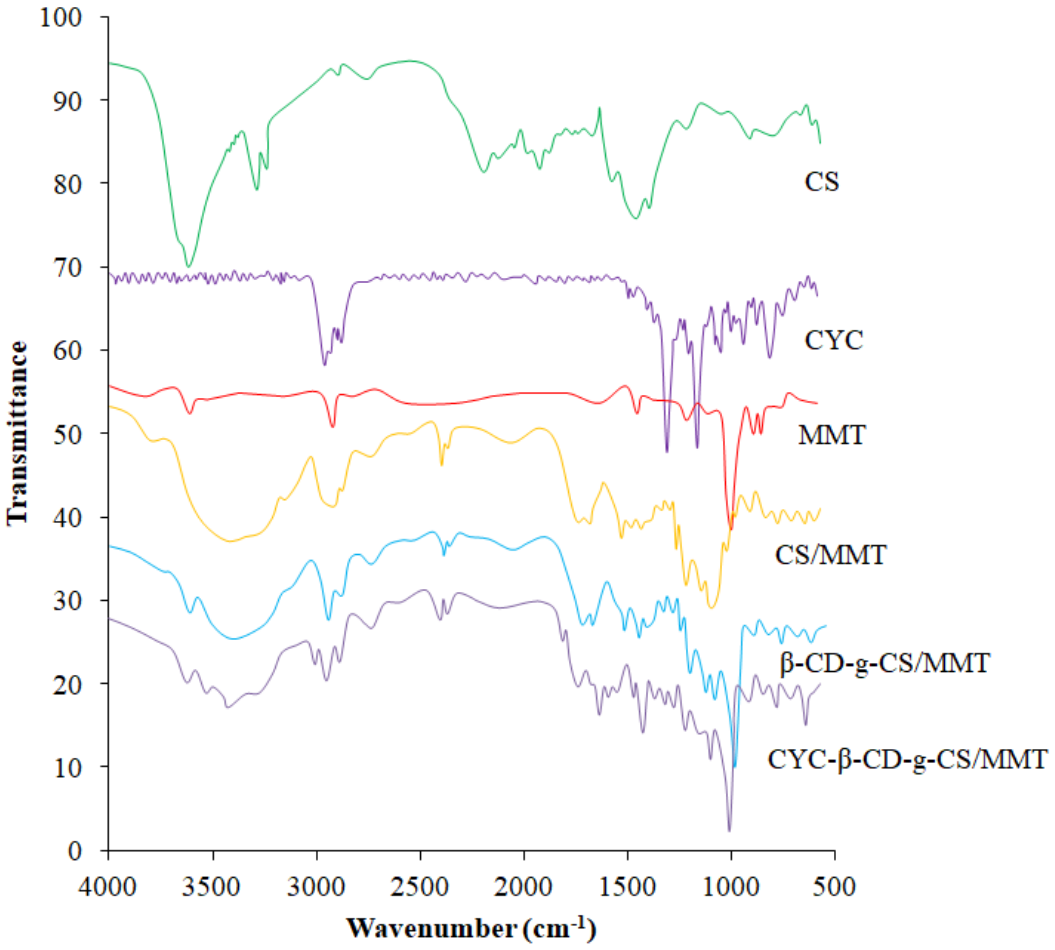

Figure 2: FTIR of CS, CYC, MMT, CS/MMT, *β*-CD-*g*-CS/MMT, CYC-*β*-CD-*g*-CS/MMT XRD

acid. The prepared solution of β-CD (5.0 g) in 40 ml N, Ndimethylformamide (DMF) was added into nanocomposites (CS/MMT). The reaction mixture of solution was refluxed at 100°C for 12 hours and dialyzed

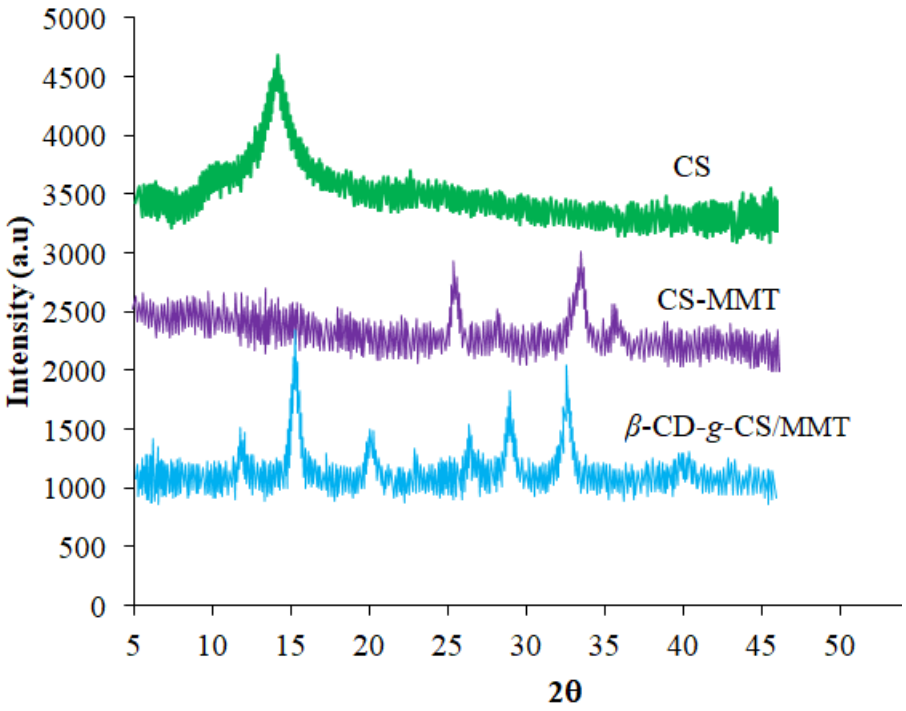

Figure 3: XRD of CS, CYC, MMT, CS/MMT, *β*-CD-*g*-CS/MMT, CYC-*β*-CD-*g*-CS/MMT SEM.

with distilled water. Then the mixture of solution was lyophilized for preparation of β-CD-g-CS/MMT powder.

Preparation of CYC drug-loaded β-CD -g-CS/MMT (β-CD -g-CS/MMT -CYC)

Different masses of Cyclophosphamide (0.05, 0.1, 0.15 and 0.2 g) were dissolved with CH modified MMT sample, which was prepared under the optimum conditions of temperature and concentrations[12]. The mixture was subjected to a magnetic stirring at different reaction temperatures (40ºC, 50ºC, 60ºC and 70ºC) for different times (0.5, 1, 2 and 4 h) to affect cross-linking.

Characterization

Fourier transforms infrared (FTIR spectra)

The FTIR spectra were demonstrated on a Nicolet 8700 spectrometer, in the absorbance range in between 400–4,000 cm^1.

X-ray diffraction (XRD)

XRD instrument Rigaku, D/Max, 2,500 V, Cu-αa radiation: 1.54056A° was used for experiment. The result was recorded at temperature of 30^0C.

Scanning Electron Microscopy (SEM)

SEM of nanocomposites was demonstrated by S 4300 Hitachi, Illinois, USA. The prepared sample was placed into a specimen holder with silver plate coated by palladium. At analysis time the accelerator potential was 10kV.

TGA

TGA was performed on a thermal analyser (TA Instruments, SDT Q600) from 40–800^{0}C at a heating rate of 10^0C/min under nitrogen atmosphere.

Differential scanning calorimetry (DSC)

DOX, CYC and CUM drugs were recorded on Perkin Elmer DSC model in nitrogen atmosphere at a heating rate of 10 ^{0}C per minute. The selected nanocomposites amount (4–5 mg) was subjected to repeat cooling and heating cycles between room temperature and 175^0 up to 300^0C.

Swelling studies

This study was performed in both simulated gastric Fluid (SGF) and (simulated intestinal fluid (SIF) in phosphate buffer (PBS) at 37^0C on copolymer pellets (100 mg, 2.55 mm thickness and 13 mm diameter). The sample was 25mm diameter; 50 mm height which was immersed 20ml phosphate buffer. The weights of the swelled sample at predetermined time intervals were calculated after wiping the mesh containing the swelled polymer with a tissue paper. Then a graph was drawn between the degree of swelling (= $(W_t-W_0)/W_0$) and time, where W_t and W_0 are the weights of the sample after and before swelling, respectively.

In vitro drug dissolution study

In vitro drug dissolution study was made by Veego Model in SGF and SIF at room temperature with 500 RPM. The amount of model drug released was estimated by UV spectrophotometer in different time interval. The absorbance of pure CYC drug was calculated to be 254 nm.

Statistical analysis

The experimental data are measured by one-way analysis of variance (ANOVA). All data analysis was executed using the SPSS Statistics 17.0. All experimental data were introduced as a mean value with its standard deviation (mean ± SD). *P*-values less than 0.05 were recommended to be statistically significant.

RESULT AND DISCUSSION

As shown in Fig. 1, chitosan was first reacted with MMT in the presence of acetic acid to functionalize partial amino groups of the chitosan with MMT. Then CS/MMT was reacted with *β*-CD in the presence of acetic acid to

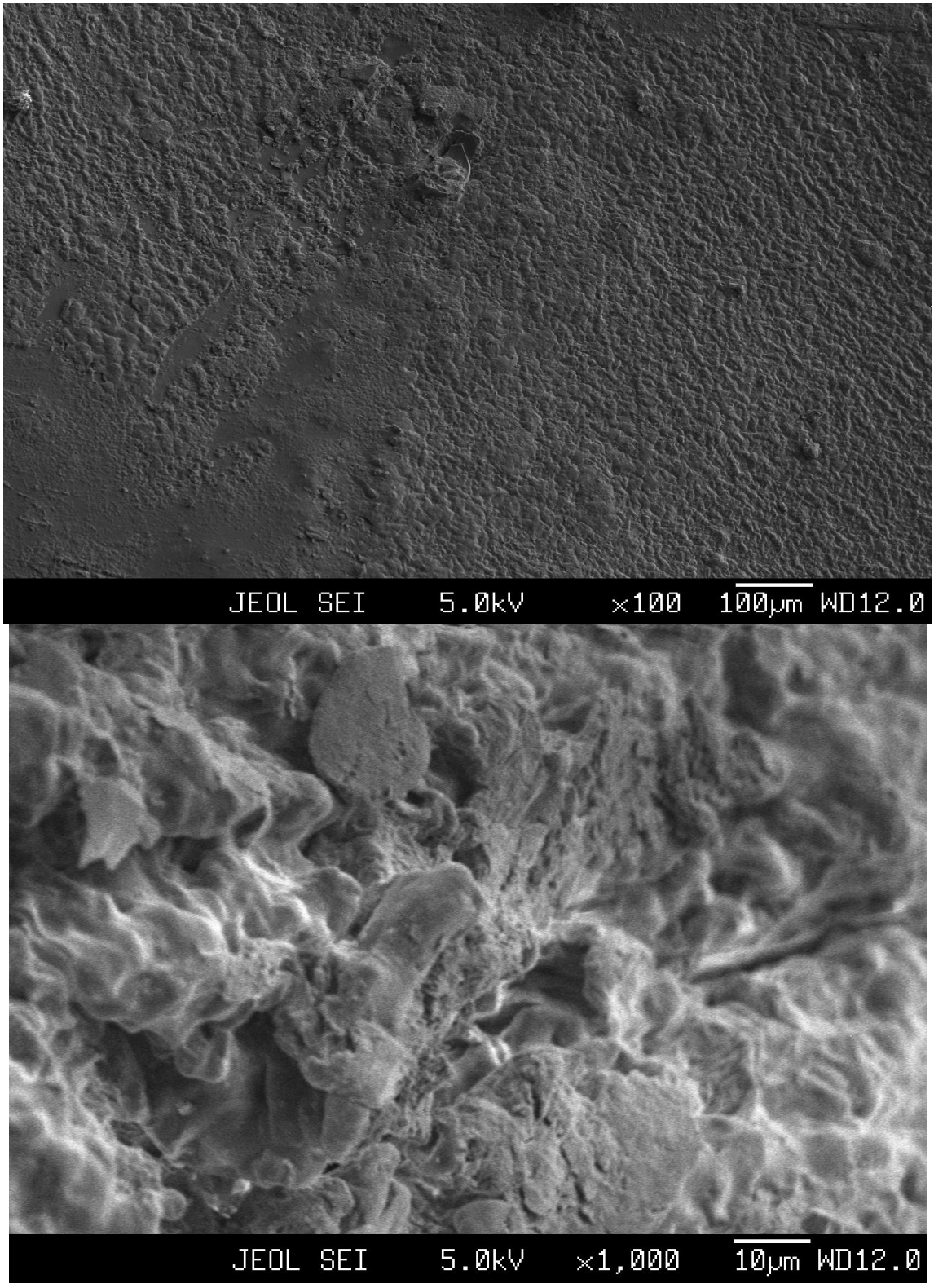

Figure 4: SEM of CS/MMT, *β*-CD-*g*-CS/MMT

functionalize partial amino groups of the chitosan with *β*-CD and obtained CD-*g*-CS/MMT.

FTIR of β-CD-g-CS/MMT

Fig.2 showed FTIR of pure CS, a broad -OH stretch absorption band between 3500 and 3100 cm^{-1} and the aliphatic C-H stretch between 2990 and 2850 cm^{-1}. The peak at 1384 cm^{-1} represented the -C-O stretch of primary alcoholic group ($-CH_2-OH$)[13].

Fig.2 showed FTIR of CS/MMT, the broad peak at 3449cm^{-1} (interlayer and interlayer H-bonding upon stretching), 3619 cm^{-1} (O-H stretching), 1633 cm^{-1}(O-H bending), 520–560 cm^{-1} (Si-O bending vibrations), 1134 cm^{-1} (Si-O stretching vibrations). At 1555 cm^{-1}

(protonated amine group) of CH is transformed towards the lower frequency value which was indicates an electrostatic interaction between amino group of CS and the negatively charged sites in the MMT structure[14].

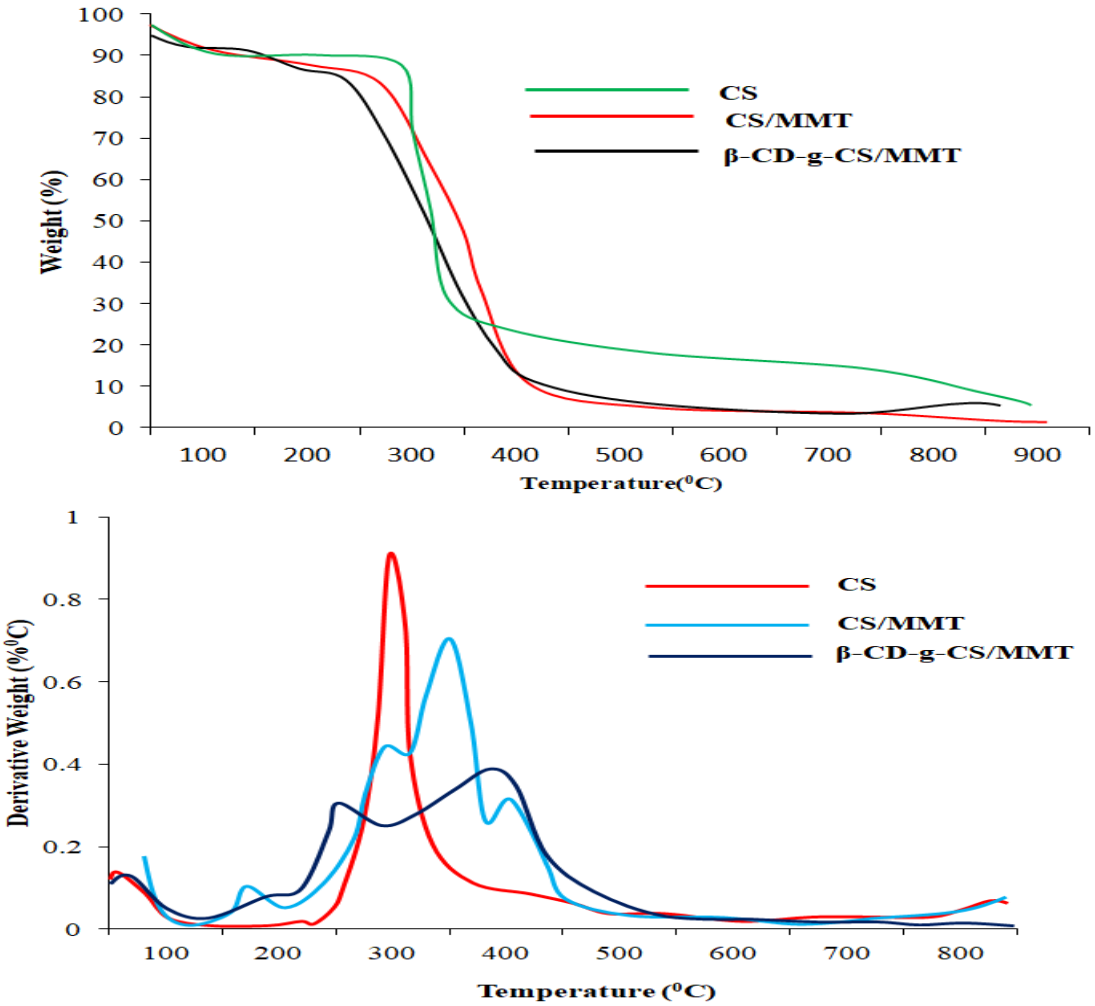

Figure 5 a: TGA of CS, CS/MMT and *β*-CD-*g*-CS/MMT, b: TG traces of CS, CS/MMT and *β*-CD-*g*-CS/MMT.

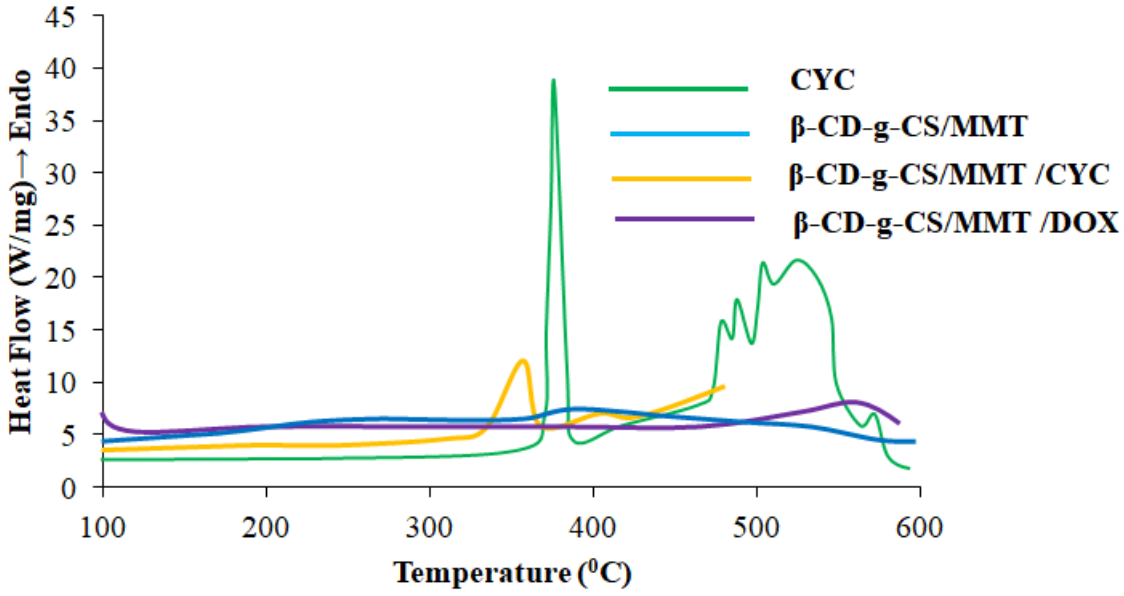

Figure 6 : DSC of CYC, *β*-CD-*g*-CS/MMT, *β*-CD-*g*-CS/MMT/cyc, *β*-CD-*g*-CS/MMT/DOX.

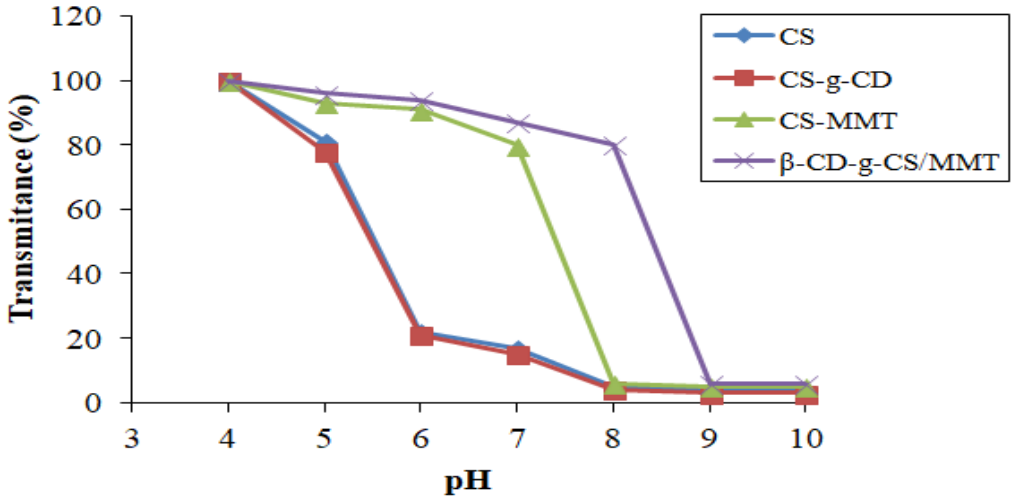

Figure 7: Solubility study of CS, CS/MMT, CS-g-CD, *β*-CD-*g*-CS/MMT.

The *β*-CD-*g*-CS/MMT showed both patterns of CS/MMT and *β*-CD. The expected peaks of chitosan backbone was at 3417 cm^{-1} and 1384 cm^{-1} (-OH stretching and -C-O stretching), respectively. Further, the absorption peak of the *β*-pyranyl vibration of chitosan at 894.9 cm^{-1} and the characteristic peak of the α-pyranyl vibration of *β*-CD at 942.8 cm^{-1} both appeared. The peak at 890 cm^{-1} was the characteristic bands of α-(1, 4) glucopyranose in *β*-CD.

Fig.3 showed XRD of pure CS, a characteristic peak at 2θ = 20.95° and MMT shows a peak at 2θ = 8.54° in Figure.2b[13]. Compared with chitosan, XRD spectra of CD-*g*-CS and CD-*g*-CS/MMT showed broad single peak pattern at 2*θ* values of 26° and 24°, respectively, indicating low crystallinity and considerably more amorphous than chitosan. It can be hypothesize that the reduced crystallinity of CD-*g*-CS and CD-*g*-CS/MMT is due to deformation of the strong hydrogen bonds in the chitosan backbone as the amino groups are functionalized by *β*-CD[14].

As shown in Fig. 4, CS/MMT a nanocomposite was studied by SEM. Pure CS has a smooth surface[15]. However, SEM images introduced the presence of CS was intercalated structures present due to the interaction of MMT nanoclay within the polymer composite. Similarly the intercalated structure was found in *β*-CD-*g*-CS/MMT nanocomposites due to the electrostatic interaction of *β*-CD and CS/MMT, respectively.

TG and DTG

TG and DTG thermograms of CS and CD-*g*-CS/MMT recorded in nitrogen atmosphere are displayed in Fig. 5a and b, respectively. The weight losses around 100^0 C in CS and CD-*g*-CS/MMT are assigned to loss of volatile impurities and moisture. The TG/ DTG of graft copolymer displayed three step degradation in the temperature range 150^0–600^0c. The weight loss in the temperature range 250^0–400^0 C with maximum weight loss around 289^0 C (51.34%) is attributed to chitosan back bone degradation[14]. The weight loss around 170^0 C is more likely to be attributed to degradation of CD fragment on the CS back bone with terminal double bonds. The weight losses observed around 280^0 and 380^0 C are due to onset degradations of CS moiety, and poly CS residue with saturated terminal ends and CS moiety, respectively. A degradation step noticed around 430 C in CS not seen in the copolymer and the observed residual weights of 8.1% and 1.6% at 830^0 C in the TG traces of CS and CS and CD-*g*-CS/MMT, respectively, collectively reveals that the graft copolymer with a decreased thermal stability degrades faster compared to CS. This was also corroborated by the residual mass of 7.1% at 830^0 C in the TG traces of the polymer blend of CS and CD-*g*-CS/MMT (Fig. 5a and b). The degradation behavior of the blend, CS and the graft copolymer are quite different indicating that the TG traces of graft copolymer displayed is not a physical mixture of CS and the homopolymers. Different thermal degradation behavior of the graft copolymer compared to that of the blend also revealed that the grafting had occurred[16,17].

DSC

Typical DSC traces for CYC and CUM drugs are displayed in Fig. 6. It is reported that the glass transition temperature (Tg) for CS was in the range 146–150 C. T g of CD-*g*-CS/MMT was not visible in the DSC[14,18]. But the melting endothermic peaks of the drugs in the matrix are quite visible. The melting points of pure drugs CYC and CUM determined by DSC were 183.25^0 and 288.77^0 C, respectively. But in the tablets they were reduced to 177.77 and 280.14^0 C, respectively. Moreover, the narrow melting endothermic peaks of the pure drugs become broadened at the base of the peak with a reduction in the onset of melting temperature (Fig. 5b and c)[19]. This tend to imply the existence of weak interaction of the drug with the matrix at a scale >100 nm[20,21].

Solubility study

Fig. 7 exhibited the transmittance of CD-*g*-CS/MMT in water with various pH compared with chitosan and CD-*g*-CS at 5 mg/ml. It was found out that the water solubility of chitosan, CD-*g*-CS and CD-*g*-CS/MMT decreased with the increase of pH. Chitosan, CD-*g*-CS, CD-*g*-CS/MMT showed excellent water solubility at low pH due to protonation of amino groups. At the pH range of 5.0–8.0, the CD-*g*-CS/MMT showed better water solubility than

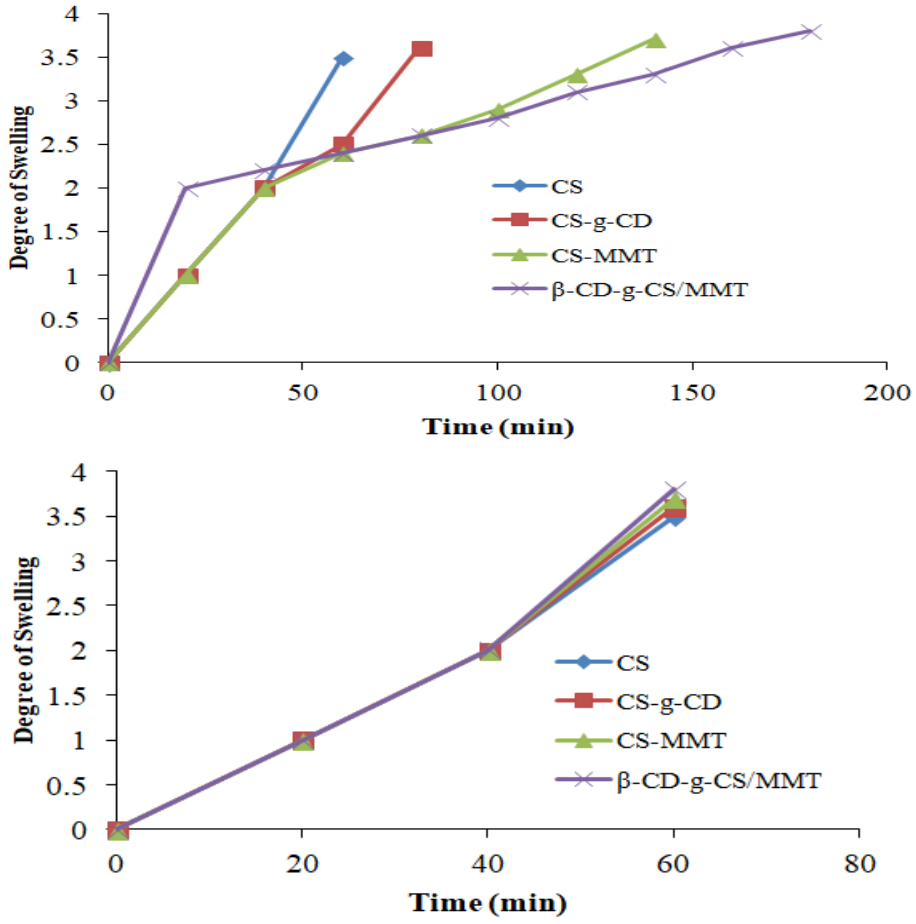

Figure 8: Degree of swelling of graft copolymer in SGF (a) and SIF (b) at 37^0 C.

chitosan and CD-*g*-CS, which indicated enhances the solubility of chitosan.

In vitro swelling studies

The ability of a drug carrier to preserve water is an important aspect to be investigated for drug delivery applications. To evaluate this effect, swelling studies were carried out with CS/MMT and CD-*g*-CS/MMT in SGF and SIF at 37^0C[15]. The degree of swelling in SGF and SIF for CD-*g*-CS/MMT polymers prepared with increasing concentrations of is given in Fig. 8a and b. The degree of swelling was significantly different in SIF and SGF for a matrix of typical composition. In SIF, the rate of swelling is more than that in SGF, and it attains the equilibrium value within 45 min. But in SGF the equilibrium swelling rate was attained only after 160 min. The greater extent of swelling in SIF compared to that in SGF may be more likely due to enhanced hydrogen bonding between CD-*g*-CS/MMT and SIF through the formation of carboxylate anion (–COO). This may also be due to lesser amount of free water molecules in SGF because of the localization of water on pepsin by secondary bond forces. At acidic pH < 2 the majority of the base and acid groups exist in $–NH^{3+}$ and –COO or $–NH_2$ and –COOH forms, and therefore ionic interaction of $–NH_3^+$ and –COO species and hydrogen bonding between amine and carboxylic acid lead to decreased swelling for samples. For pH values > 7 swelling may increase again due to the dissociation of ionic cross linking and the repulsive interaction between negatively charged carboxylic groups[22]. But the initial fluid uptake was rapid in both the fluids due to H-bonding interaction via the carboxylic acid group.

In vitro drug dissolution study

CD-*g*-CS/MMT matrices were synthesized with various concentrations of CD in the feed. Both in SIF and SGF the drug release rate was greater for pure CS than that observed for grafted CS/MMT[15]. This was attributed to the burst release of the drugs due to tablet breaking after immersing in biofluids. For the same drug, the release rate is more in SIF than in SGF (Fig. 9a). This is more likely attributed to the greater degree of swelling of the matrix in SIF than in SGF. But grafting decreased the drug release in both the fluids. This is more likely attributed to the enhanced drug–polymer interaction through H-bonding between –COOH and –OH groups of CD-*g*-CS/MMT and –OH group of the drug as supported by DSC (Fig. 6). With CS as carrier, 80–85% of drug was released in SIF for the initial 30 min and this decreased to 60% with CD-*g*-CS/MMT matrix. But in SGF these figures were 70% and 10%, respectively. It took roughly 120 min for 60% release of drug in SGF. As in the case of swelling studies, increased concentration of CD in the feed increased the drug release rate with the corresponding copolymer matrix as carrier perhaps due to enhanced swelling and hence increased diffusion of dissolved drug CYC which is highly

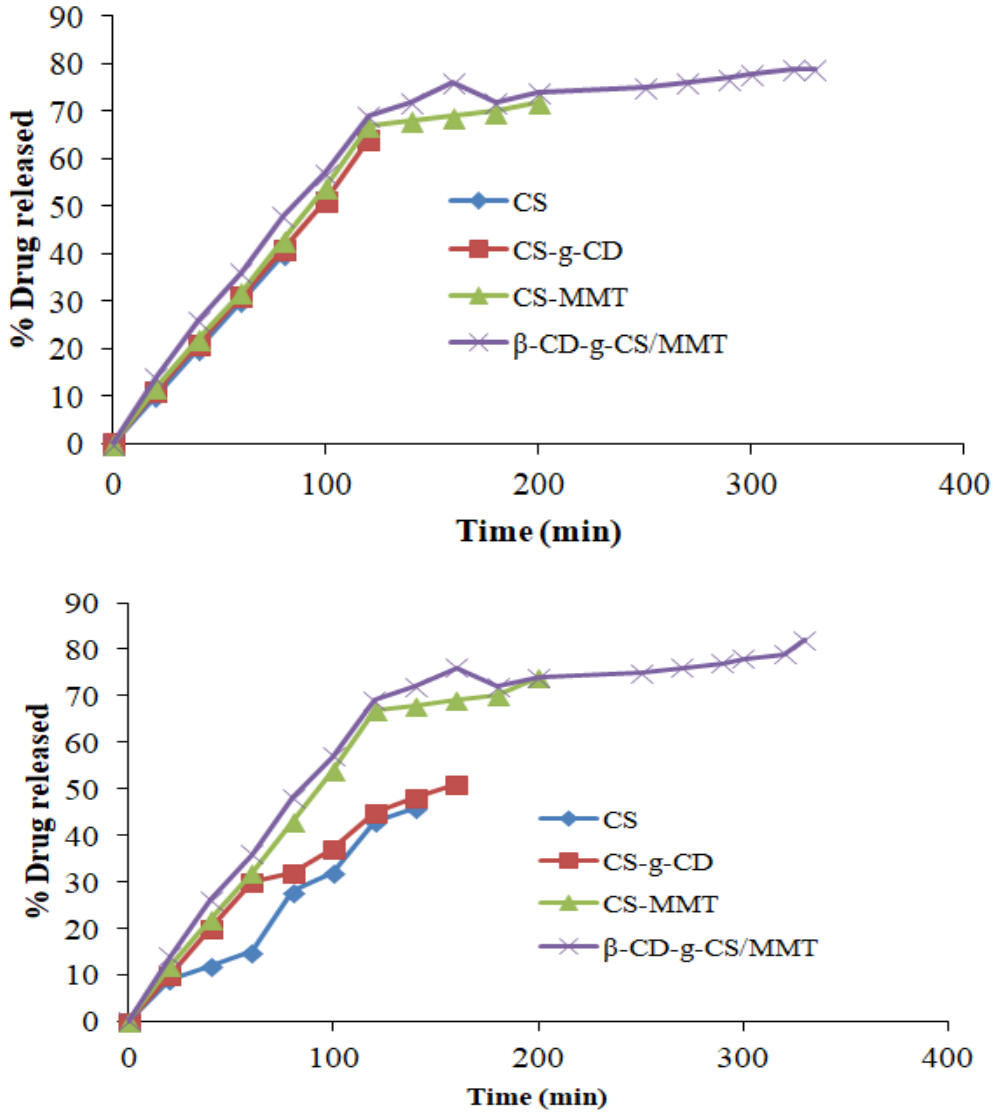

Figure 9: Release profiles of model drug CYC (A) and of CYC, DOX, CUM drugs (B) in SGF and SIF at 37^0C, with graft copolymer carriers CS, CS/MMT, CS-g-CD, *β*-CD-*g*-CS/MMT.

water soluble. Increasing the CD content in polymer will facilitate enhanced fluid-polymer interaction through H-bonding during swelling. In SIF, the carboxylic groups will be in the ionized state and it opens up the structure. In this time, the CS could be in the precipitated condition. These opposing factors will have a net effect on the release of the incorporated drug.

Comparison of the typical release profiles of CUM, CYC, DOX in the copolymer carrier of a typical composition demonstrated (Fig. 9b) the effect of chemical structures of drugs on their release kinetics. The release rates for these drugs in SGF and SIF were in the order, DOX > CYC> CUM both in SIF and SGF. The higher release rates for the drugs DOX and CYC which are bulkier than CUM may be attributed to their higher solubilities in aqueous medium. The lowest release rate for CUM is more likely attributed to the drug–matrix interaction through H-bonding in the swollen tablet involving phenolic –OH of CUM and its lower water solubility.

Drug release mechanism

To understand and analyze the mechanism of in vitro drug release from nanocomposites by Korsmeyer–Peppas's equation[23,24] viz.,

$M_t/M_\infty = kt^n$

Where M_t/M_∞ is the fractional release of drug at time't' or fractional uptake of fluid in swelling in the absence of drug (M_t/M_∞, amounts of model drug released at time 't' respectively) was used. The release mechanism of drug was explained by Peppas equation. The slope of the linear plot log M_t/M_∞ versus log t, for drug release < 50% gives the power law exponent (n) value. The equation n = 0.5 (diffusion-Fickian controlled drug release) and n = 1 (swelling-controlled drug release or non-Fickian) where is 'n' anomalous transport kinetics. The observed 'n' values for typical release profiles of DOX, CYC and CUM were <0.5, >0.5 and > 1.0. These ranges of 'n' values indicate a combined mechanism of pure diffusion and non-Fickian for the drug release with the grafted chitosan matrix both in SGF and SIF. The same drug release mechanism was implicated with virgin CS as a carrier also. This

mechanism may also be partly due to the weak physical interaction of the polymer matrix with drug at scales > 100 nm as indicated by the DSC studies on the tablet and the drug.

CONCLUSIONS

CD-*g*-CS/MMT has been synthesized and characterized for controlled released of CYC for oral drug delivery. The drug release rate was greater in SIF than in SGF due to enhanced matrix swelling in SIF and lower with CD-*g*-CS/MMT carrier compared to CH. In SGF the initial drug release rate was sluggish but started increasing rapidly after 40 min due to increased segmental mobility. Increasing the concentration of CD in the feed enhanced the drug release rate with the corresponding grafted CS as carrier due to enhanced polymer–biofluid interaction. For a graft copolymer of specific composition the release rates of DOX, CYC and CUM follows the order DOX > CYC > CUM both in SIF and SGF implying the effect of chemical structures on the rate of drug release. The higher release rates for DOX and CYC may be attributed to their higher solubilities in SBF. The lowest release rate for CUM is more likely attributed to the drug–matrix interaction through H-bonding and its lower water solubility. The observed values (0.5–2.2) of power law exponents indicated a mixed pure diffusion and non-Fickian mechanisms for drug release in simulated biological fluids.

REFERENCE

1. Majeti N.V., Ravi Kumar, A., review of chitin and chitosan applications, Reactive and Functional Polymers, 46(1), 2000, 1-27
2. Marguerite Rinaudo, Chitin and chitosan: Properties and applications, Progress in Polymer Science, 31(7),2006, 603-632
3. Chen YZ, Huang YK, Chen Y, et al. Novel nanoparticles composed of chitosan and β-cyclodextrin derivatives as potential insoluble drug carrier. Chin Chem Lett 2015;26:909-913.
4. Ye YJ, Wang Y, Lou KY, et al. The preparation, characterization, and pharmacokinetic studies of chitosan nanoparticles loaded with paclitaxel/dimethyl-β-cyclodextrin inclusion complexes. Int J Nanomed 2015;10:4309-4319.
5. Yang Y, Gao J, Ma X, et al. Inclusion complex of tamibarotene with hydroxypropyl-β-cyclodextrin: preparation, characterization, in-vitro and in-vivo evaluation. Asian J Pharm Sci 2016;12:187-192.
6. Matsubara K, Ando Y, Irie T, et al. Protection afforded by maltosyl-beta-cyclodextrin against alphachymotrypsin-catalyzed hydrolysis of a luteinizing hormone-releasing hormone agonist, buserelin acetate. Pharm Res 1997; 14: 1401-1405.
7. Manakker FVD, Vermonden T, Nostrum CFV, et al. Cyclodextrin-based polymeric materials: synthesis, properties, and pharmaceutical/biomedical applications. Biomacromolecules 2009;10: 3157-3175.
8. Maestrelli F, González-Rodríguez ML, Rabasco AM, et al. Effect of preparation technique on the properties of liposomes encapsulating ketoprofen–cyclodextrin complexes aimed for transdermal delivery. Int J Pharm 2006;312:53-60
9. Petter RC, Salek JS, Sikorski CT, et al. Cooperative binding by aggregated mono-6-(alkylamino)-betacyclodextrins. J Am Chem Soc 1989;112:3860-3868.
10. Yuan ZT, Ye YJ, Gao F, et al. Chitosan-graft-β-cyclodextrin nanoparticles as a carrier for controlled drug release. Int J Pharm 2013;446:191-198.
11. Ebru Günister, Dilay Pestreli ,Cüneyt H. Ünlü ,Oya Atıcı, NurferGüngör , Synthesis and characterization of chitosan-MMT biocomposite systems, Carbohydrate Polymers, 67(3), 2007, 358-365
12. Shahrzad Fathollahipour,Ali Abouei Mehrizi,Azadeh Ghaee,Mojtaba Koosha, Electrospinning of PVA/chitosan nanocomposite nanofibers containing gelatin nanoparticles as a dual drug delivery system, Journal of biomedical materials research, 103(12), 2015 , 3852–3862
13. Suneeta Kumari, Pradip Kumar Rath, Extraction and Characterization of Chitin and Chitosan from (Labeo rohit) Fish Scales,Procedia Materials Science,6, 2014, , 482-489
14. Ebru Günister, DilayPestreli Cüneyt H.Ünlü OyaAtıcı Nurfer Güngör, Synthesis and characterization of chitosan-MMT biocomposite systems, , Carbohydrate Polymers, 67(3), 2007, 358-365
15. Garima Thakur, Amrinder Singh, and Inderbir Singh, Chitosan-Montmorillonite Polymer Composites: Formulation and Evaluation of Sustained Release Tablets of Aceclofenac, Sci Pharm. 2016; 84(4): 603–618.
16. Naguib, H.F., 2002. Chemically induced graft copolymerization of itaconic acid onto sisal fibers. J. Polym. Res. 9, 207–211.
17. Isiklan, N., Kursun, F., Inal, M., 2010. Graft copolymerization of itaconic acid onto sodium alginate using benzoyl peroxide. Carbohydr. Polym. 79, 665–672
18. Argin-Soysal, S., Kofinas, P., Lo, Y.M., 2009. Effect of complexation conditions on xanthan–chitosan polyelectrolyte complex gels. Food Hydrocolloids 23, 202–209
19. Singh, D.K., Ray, A.R., 1994. Graft copolymerization of 2-hydroxyethyl methacrylate onto chitosan films and their blood compatibility. J. Appl. Polym. Sci. 53, 1115–1121.
20. Cheung, M.K., Wang, J., Zheng, S., Mi, Y., 2000. Miscibility of poly (epichlorohydrin)/ poly (vinyl acetate) blends investigated with high-resolution solid-state 13C NMR. Polymer 41, 1469–1474.
21. Manley, R.St.J., 1998. Blends of cellulose and synthetic polymers. Cellulose derivatives. ACS Symp. Ser. 688, 253–264 (Chapter 18)

22. Milosavljevic, N.B., Milasinovic, N.Z., Popovic, I.G., Filipovic, J.M., Krusic, M.T.K., 2011. Preparation and characterization of pHsensitive hydrogels based on chitosan, itaconic acid and methacrylic acid. Polym. Int. 60, 443–452
23. Korsmeyer, R.W., Meerwall, E.V., Peppas, N.A., 1986. Solute and penetrant diffusion in swellable polymers. II. Verification of theoretical models. J. Polym. Sci., Part B: Polym. Phys. 24, 409–434.
24. Ritger, P.L., Peppas, N.A., 1987. Simple equation for description of solute release II. Fickian and anomalous release from swellable devices. J. Control Release 5, 37–42.